Femtosecond laser induced periodic large-scale surface structures on metals

Xiangming Dong (董祥明), Haiying Song (宋海英), and Shibing Liu (刘世炳)*

Strong-Field and Ultrafast Photonics Lab, Institute of Laser Engineering,
Beijing University of Technology, Beijing 100124, China
**Corresponding author: sbliu@bjut.edu.cn*

Received March 19, 2015; accepted April 29, 2015; posted online June 4, 2015

The periodic ripple structures on wolfram and titanium surfaces are induced experimentally by linear polarized femtosecond laser pulses at small incident angles. The structural features show a material difference in the *s*- and *p*-polarized laser irradiation. The interspace between the ripples increases significantly for *p*-polarized laser irradiation when it exceeds a threshold angle, and the ripples' periodicities are larger than the wavelength of the incident *p*-polarized femtosecond laser; however, no significant change in the period of the ripples is observed with increasing incident angle for *s*-polarized laser irradiation. To explain these phenomena we propose a resonant absorption mechanism, by which the experimental observations can be interpreted.

OCIS codes: 100.0118, 180.0180, 350.0350.
doi: 10.3788/COL201513.071001.

Femtosecond (fs) laser-induced periodic surface ripple structures (LIPSSs) deviating significantly from the predicted period which is less than the incident laser wavelength have been extensively studied at a variety of metal materials by changing the parameters of the laser[1–6]. Meanwhile, the ripples usually orientate in a manner that is perpendicular to the polarization direction of the laser light. Recent studies showed that the interference between the incident laser light and the surface scattered wave explains the formation of ripples[7–9]. It is proposed that the surface plasmon polaritons excited by fs laser irradiation play a crucial role in the formation of ripples[10–12].

More recently, nanostructure-covered (NC) large-scale waves (LSWs) with a period of tens of times greater than the laser wavelength have been studied using an oblique incidence laser at high fluence[13–17]. The morphology of this LSW pattern has a close dependence on the laser fluence and the number of laser pulses, but not on the laser wavelength. It is suggested that this LSW is initiated by fs-laser-induced surface unevenness followed by periodically distributed nonuniform surface heating from fs pulse irradiation[14]. The structure has been discussed for different polarization states at large incident angles and a three-step model has been established for the NC–LSWs[16]. Although the aforementioned interpretation has been given in the context of the formation of the NC–LSWs, how to comprehensively understand different polarizations induced by a fs-laser-induced ripple is still unknown at small incident angles.

In this work, a threshold angle for the formation of large-scale periodic ripple structures induced by an oblique incident *p*-polarized fs laser pulse on the surfaces of wolfram (W) and titanium (Ti) metals is found experimentally. The dependences of incident angle and laser fluence on the formed ripple period are demonstrated by changing the polarization directions of the incident laser. To interpret these threshold effects and the dependences for the self-formation of ripple periods, we propose a resonance absorption mechanism resulting from the interaction of a *p*-polarized fs lasers and plasma.

The experimental system used for this work is presented in Fig. 1. The laser used in the work is an amplified Ti:sapphire fs laser system, which provides 35 fs pulses of an energy of 3 mJ/pulse operated at a 1 kHz repetition rate at a central wavelength of 800 nm. The beam power profile is Gaussian. The fluence of the incident fs laser is controlled using attenuators. A half-wave plate is used to change the polarization of the fs laser beam before the laser beam is focused by the lens. The pulse numbers are controlled by an electromechanical shutter. For each iteration, a train of 100 laser pulses is focused onto the samples. The samples are Ti and W foil with thickness of 10 mm prepared by mechanically polishing the surface. First, to produce the ripple structure, a train of 100 *s*- and *p*-polarized fs laser pulses is weakly focused onto Ti at am incident between 0° and 35° with a resolution of 5°, respectively, and we change the laser pulse energy to keep the same laser fluence on the sample surfaces to be constant at each incident angle (θ). Second, to study the influence of the fluence on the threshold angle, larger-scale ripples are produced at a different fluence by a *p*-polarized fs laser irradiated on Ti and W, and we refine incident angles between 13° and 20° with an interval of 1°, which are controlled by rotating a stage on which the samples are vertically mounted. Using a lens with a focal length of 150 mm and a focal area of 10 μm at the normal, the beam size of the laser output is 8 mm. Our entire work was performed in air. To study the detailed texture of the ripples, the ripples were imaged using a scanning electron microscope (SEM), and the SEM images are taken from the central position of the ablating spot.

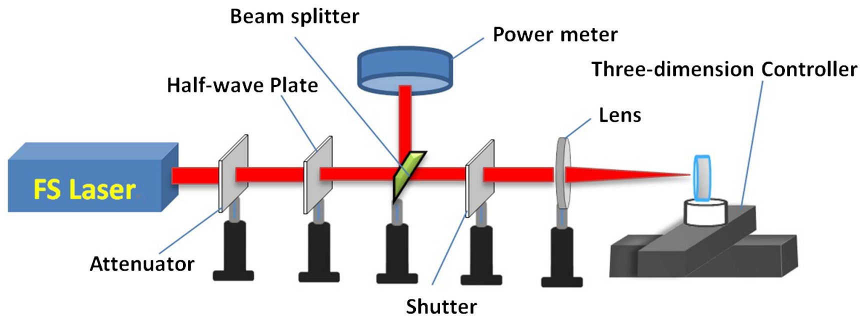

Fig. 1. Schematic diagram of the experimental setup.

Figures 2(a)and 2(b) show the SEM images of ripples that are produced on Ti by 100 pulses of irradiation with a fluence of 0.1 J/cm^2 at incident angles of 0°, 20°, and 30°, respectively, using two polarizations, *p*- and *s*-polarized. The period of the ripples was between two neighboring ripples estimated from the SEM pictures. As observed, when the incident angle is less than 20°, with increasing incident angle of a *p*-polarized fs laser pulse, the change of the ripple periodicity is not obvious, and less than the wavelength of the incident laser. However, when the incident angle is $\theta = 20°$, the ripple periodicity will increase significantly, and is more than the wavelength of the incident fs laser. If the laser incident angle increases further, the ripple periodicity becomes even larger. Instead, with increasing incident angle, no significant change in the period of the ripples is observed for *s*-polarized light, and the ripple periodicities are less than the wavelength of the incident fs laser. Based on our experimental results in Fig. 3, at a given laser fluence, when the incident laser angle with *p*-polarized exceeds a threshold angle, the ripples periodicities will be larger than the wavelength of the incident fs laser.

Next, we study the dependence of the threshold angle on the fluence of a *p*-polarized fs laser; the fluence of an incident fs laser through a *p*-polarized fs laser beam incident onto a Ti surface at a fluence of $F_1 = 0.2$ J/cm^2, $F_2 = 0.4$ J/cm^2, and $F_3 = 0.6$ J/cm^2. The results of this dependence are plotted in Fig. 4. The ripples' periodicities increase. When the incident angles are 14°, 15°, and 17°, the ripple periodicities increase suddenly and the periods are 913.7, 935.5, and 913.5 nm, respectively, as shown in Fig. 4. Basing on the aforementioned results, there is the threshold angle; when the incident angle of the laser exceeds it, the ripple periodicities will increase drastically and become larger than the wavelength of the incident

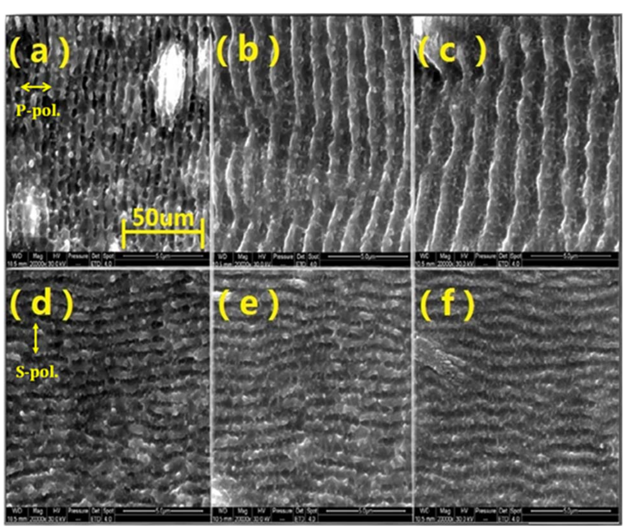

Fig. 2. SEM images of ablation Ti at a fluence of 0.1 J/cm^2 and incident angles of 0°, 20°, and 30°: (a)–(c) *p*-polarized fs laser; (d)–(f) *s*-polarized fs laser.

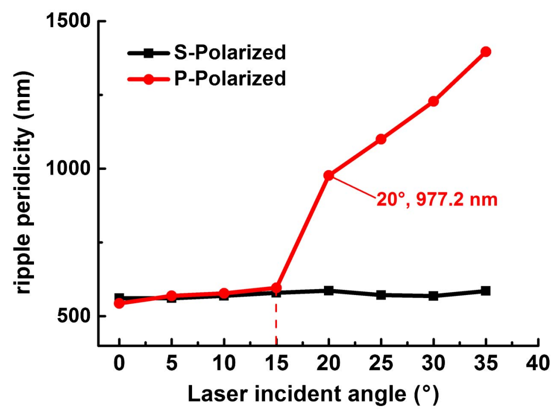

Fig. 3. Dependence of LIPSS period on a variety of irradiating *p*- and *s*-polarized incident angles at a fluence of 0.1 J/cm^2 on Ti.

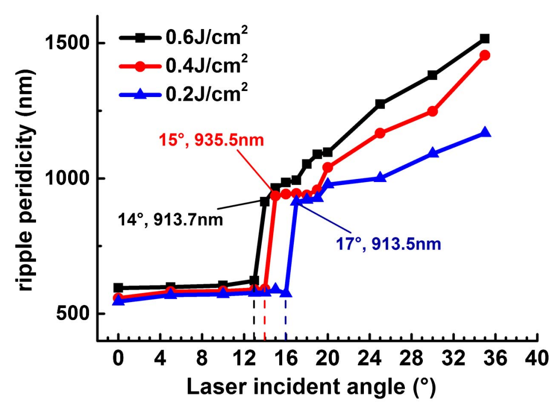

Fig. 4. Dependence of ripple periodicity with *p* polarization on the incident laser angle at fluences of 0.6, 0.4, and 0.2 J/cm^2 irradiating on Ti.

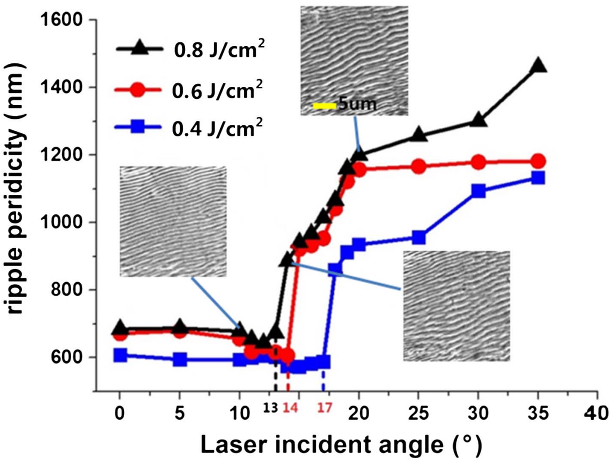

Fig. 5. Dependence of ripple periodicity with p polarization on the incident laser angle at fluences of 0.8, 0.6, and 0.4 J/cm^2 on a W surface. Insets, ripples' images of the selected data points.

laser. With increasing incident angle of the p-polarized fs laser, the threshold angle reduces. Subsequently, the thresold angle was also found during p-polarized fs laser irradiation on a W surface. As shown in Fig. 5, when a W surface is irradiated by a train of 100 p-polarized laser pulses at fluences of $F_1 = 0.8\ \mathrm{J/cm^2}$, $F_2 = 0.6\ \mathrm{J/cm^2}$, and $F_3 = 0.4\ \mathrm{J/cm^2}$, the threshold angles are observed 13°, 14°, and 17°, respectively. Based on the aforementioned results, on the one hand, there are the thresold angles by a p-polarized fs-laser irradiating on a different metal. On the other hand, at the given laser fluence, the threshold angles of W are larger than Ti. In contrast, the fluence of the laser with irradiation on the W surface is higher than Ti at the same threshold angle.

In the following, we discuss the origin of the threshold angle. According to a previous study[17,18], the oblique incident p-polarized fs laser exists the component of the electric vector which oscillates electrons along the direction of the density gradient; i.e, $\mathbf{E} \cdot \nabla n_e \neq 0$ ($\mathbf{E_z}$), where n_e is the electron density. Since this oscillation generates fluctuations in charge density that are enhanced resonantly by the plasma, the wave is no longer purely electromagnetic[18,19]. The partial energy of the incident fs laser wave is transferred to an electrostatic oscillation. This phenomenon is known as resonance absorption. To our knowledge, regarding fs laser irradiation on metal targets, Yang *et al.*[1] reported this observation. Additionally, there is a microscale electric plasma in close contact with the solid-state matter even during the pulse, because the free electrons are quickly heated to escape from the surface through both photoelectric and thermionic emission processes[20–22]. When the electron density n_e with the plasma layer is under-dense, the frequency of the incident laser will be larger than the relevant plasma frequency, i.e., $\omega < \omega_p$. In this case, the laser pulse can penetrate the sandwich-like air-plasma-target. Furthermore, the ionization of practically any target material takes place early in the laser pulse time at intensities above 10^{13}–$10^{14}\ \mathrm{W/cm^2}$[23]. The peak power used in the work is 5.7×10^{12} to $2.3 \times 10^{13}\ \mathrm{W/cm^2}$, which is enough to generate a dense plasma with n_e close to the critical value in contact with the metal surface. So, it is possible that the resonant absorption is induced by the incident laser interactions with the surface plasmon. Additionally, the resonance absorption is excited by the resonantly driven field $\mathbf{E_d}$[22,24]. Physically, the resonantly driven field is the component of the electric field of the light wave which oscillates electrons along the density gradient, namely: $\mathbf{E_d} \propto \mathbf{E_z}$. In addition, previous studies for regular LIPSSs suggest that the interference between the incident wave and the generated surface plasmons induces LIPSSs for metal materials[12]. Based on the aforementioned mechanism, the LIPSSs period, Λ, is given by[12]

$$\Lambda = \frac{\lambda}{\mathrm{Re}[\eta] \pm \sin\theta} \quad \text{with } \mathbf{g} \| \mathbf{E}, \tag{1}$$

where λ is the laser wavelength, θ is the incident angle of the fs laser, $\eta = [\varepsilon_1\varepsilon_2/(\varepsilon_1 + \varepsilon_2)]^{1/2}$ is the effective refractive index of the plasma–metal interface $\mathrm{Re}[\eta]$ is the real part of η, $\varepsilon_1 = 1 - \omega_p^2/\omega^2$ is the dielectric constant of the plasma, ε_2 is the dielectric constant of the metal, and ω_p is the surface plasmon frequency on metals. Term $\mathbf{g}$ is the grating vector, and $\mathbf{E}$ is the electrical field vector of the incident wave. When the incident angle is small, the component of the electric vector is neglected. So, the experimental results are similar to fs laser normal incidence and $\Lambda < \lambda$[1,8]. Once the incident angle exceeds the threshold angle, the resonantly driven field $\mathbf{E_d}$ will meet the condition to induce the resonance absorption, and then the energy of the incident laser absorbed by the electors will clearly increase. In this case, the kinetic energy of the electron will be larger and the electron collision probability will increase significantly. As a result, the secondary ionization of the material will be induced. At this time, more electron density will be generated, and $\varepsilon_1 = 1 - \omega_p^2/\omega^2$ will reduce drastically due to $\omega_p \propto n_e^{1/2}$, and $\omega_p \to \omega$ ($\varepsilon_p \to 0$). Thus, according to Eq. (1), the refractive index will decrease ($\eta < 1$), and the ripple periodicity will increase ($\Lambda > \lambda$). In addition, since $\mathbf{E_z}$ is strongly peaked at the critical density, the resonantly driven field is approximated as $\mathbf{E_d}/\varepsilon_1$[25], and $\mathbf{E_Z} = \frac{\mathbf{E_d}}{\varepsilon_1}$. So, with increasing incident laser fluence, the threshold angle θ is also reduced, as seen in Fig. 4. In addition, since the resonantly driven field E_d which is driving the resonance absorption, is nonexistent for an s-polarized fs laser pulse. So, as the incident angle increases, the change in ripple periodicity is small and the periodicity is less than the wavelength of the incident fs laser. It is coincident with our experimental results.

In conclusion, through multiple trains of fs laser pulse irradiation with two polarizations, various incident angles, and fluence, ripples are created on W and Ti. We find that the incident angle exceeds a threshold angle, a significant change with ripple periodicity is observed for a p-polarized fs laser pulse, and the threshold angle decreases with increasing fluence of the incident fs laser pulse. The threshold angle of W is larger than Ti at a same fluence irradiation. However, with increasing incident angle, the ripple periodicity almost remains constant for *s*-polarized fs laser irradiation. We suggest that the polarization state plays an important role to induce the sudden increase in ripple periodicity with fs laser pulse irradiation. We propose a resonant absorption mechanism, by which the experimental observations for the resonant absorption effect can be interpreted.

This work was supported by the National Natural Science Foundation of China under Grant No. 51275012.

References

1. Y. Yang, J. Yang, L. Xue, and Y. Guo, Appl. Phys. Lett. **97**, 141101 (2010).
2. X. Jia, Y. Yuan, D. Yang, T. Jia, and Z. Sun, Chin. Opt. Lett. **12**, 113203 (2014).
3. Md. S. Ahsan, F. Ahmed, Y. G. Kim, M. S. Lee, and M. B. G. Jun, Appl. Surf. Sci. **257**, 7771 (2011).
4. M. Chen, X. Liu, Y. Liu, and M. Zhao, Chin. Opt. Lett. **10**, 051402 (2012).
5. L. Qi, K. Nishii, and Y. Namba, Opt. Lett. **34**, 1846 (2009).
6. S. Zhang, X. Hu, Y. Liao, F. He, C. Liu, and Y. Cheng, Chin. Opt. Lett. **11**, 033101 (2013).
7. T. Y. Hwang and C. Guo, J. Appl. Phys. **109**, 083521 (2011).
8. T. Y. Hwang and C. Guo, J. Appl. Phys. **108**, 073523 (2010).
9. T. Y. Hwang and C. Guo, J. Appl. Phys. **110**, 073521 (2011).
10. T. Y. Hwang and C. Guo, Opt. Lett. **36**, 2575 (2011).
11. J. E. Sipe, J. F. Young, J. S. Preston, and H. M. Van Driel, Phys. Rev. B **27**, 1141 (1983).
12. A. M. Bonch-Bruevich, M. N. Libenson, V. S. Makin, and V. V. Trubaev, Opt. Eng. **31**, 718 (1992).
13. G. S. Zhou, P. M. Fauchet, and A. E. Siegman, Phys. Rev. B **26**, 5366 (1982).
14. J. Wang and C. Guo, J. Appl. Phys. **100**, 023511 (2006).
15. J. Bonse, A. Rosenfeld, and J. Krger, J. Appl. Phys. **106**, 104910 (2009).
16. M. Huang, F. Zhao, Y. Cheng, N. Xu, and Z. Z. Xu, ACS Nano **3**, 4062 (2009).
17. A. Y. Vorobyev, V. M. Kuzmichev, N. G. Kokody, P. Kohns, J. Dai, and C. Guo, Appl. Phys. A. **82**, 357 (2006).
18. N. G. Denisow, Sov. Phys. JETP **4**, 544 (1957).
19. V. L. Ginzberg, *The Properties of Electromagnetic Wave in Plasma* (Pergamon, 1964).
20. S. Sakabe, M. Hashida, S. Tokita, S. Namba, and K. Okamuro, Phys. Rev. B **79**, 033409 (2009).
21. Z. Chen and S. Mao, Appl. Phys. Lett. **93**, 051506 (2008).
22. X. Wang and M. Downer, Opt. Lett. **17**, 1450 (1992).
23. E. G. Gamaly, A. V. Rode, and B. Luther-Davies, Phys. Plasmas **9**, 949 (2002).
24. D. Forslund, J. Kindel, K. Lee, E. Lindman, and R. L. Morse, Phys. Rev. A **11**, 679 (1975).
25. W. L. Kruer, *Laser Plasma Interactions* (SUSSP, 1980).